Piezoelectrical driven resonant force sensor: fabrication and crosstalk

K. Funk, T. Fabula*, G. Flik and F. Lärmer

Robert Bosch GmbH, Postfach 10 60 50
D - 70049 Stuttgart, Germany

* HSG - IMIT, Wilhelm-Schickard-Str. 10
D - 78052 Villingen-Schwenningen, Germany

Abstract

This paper presents a resonant force sensor comprising piezoelectric ZnO-thin-film transducers for excitation and detection of resonant beam vibrations. A short description of the processing technique is given, i.e. deposition and passivation of the ZnO layer and separation of beam structures. The electrical behavior of the sensor was optimized by patterning ZnO areas to minimize electrical crosstalk effects.

Introduction

In contrast to sensors with voltage- or current-output resonant sensors transform mechanical force (stress) directly to a frequency change. The resulting frequency shift depends only on the mechanical behaviour of the resonator. The resonance frequency of a sensor element is affected by the stress caused e.g. by the applied force [1,2]. To detect this frequency shift, the resonator must be kept in a continuous oscillation. An effective way to excite an out-of-plane vibration is the induction of a periodic bending stress by an electrically driven piezoelectric ZnO film area [4,5]. Another area of the same ZnO-film can be used to detect the resulting vibration. Driven the sensor in this way (two-port-mode), there are parasitic currents, i.e. an electrical crosstalk between the exciting area(s) and the area(s) for evaluating the vibration. This crosstalk effects the electrical behaviour of the sensor, which is important for dimensioning the electronic feedback loop (oscillator).

For measuring purposes the resonator is the frequency-control unit in this oscillator, the output signal of which is fed to a microcontroller.

Technology

The sensor process combines zinc oxide with silicon micromachining technology. Clamped-clamped silicon beams as mechanical resonators with piezoelectric drive and detection are produced by plasma trenching through thin silicon membranes left at the front side of the wafers by wet etching from the backside, after frontside processing is completely finished.

The first process step is growing a thin thermal oxide and a thin LPCVD-nitride as a masking layer. The masking layer on the frontside of the wafer is opened, before boron is implanted at a high dose (10^{19} cm^{-3}) to create ground electrodes of p^+-type conductivity. The p^+-regions mark the later piezo-electric drive and detection zones. Drive and detection ground electrodes are separated from each other for cross talk reduction. There are p^+-connections to the later ground pad regions. The backside nitride mask is opened in the same lithography step for V-groove etching the membranes at a later process stage.

After implantation, a field oxide is grown in the window areas during drive in of the dopants. The field oxide is opened afterwards to define the later zinc oxide areas and the ground contact pads at the wafer front. The oxide is also removed in the backside (nitride) windows.

Zinc oxide is then deposited over the whole wafer and directly on the p^+-silicon open areas by reactive magnetron sputtering from a zinc target in an oxygen containing argon plasma. For intermediate Ar/O_2 ratios filmstress varies almost linearly, changing from compression to tension at around 55% Ar content. Maximum piezoelectrical activity is achieved by a perpendicular c-axis orientation with respect to the substrat.

Finite element simulation leds to effective coupling factors k_{eff} at around 0.2 for a thickness ratio ($d_{Silicon}/d_{ZnO}$) near 4. These results agrees very well with the measured effective koefficients. The electrical breakthrough of Al/ZnO/p-Si is observed at 10V/µm. ZnO as a II-VI compound semiconductor forms a n-ZnO/p-Si-Heterostructure diode when deposited on the p^+-silicon surface.

The zinc oxide is then wet etched in an acidic solvent to form the piezoelectrically active regions.

Aluminium is deposited and structured on top of the zinc oxide; an alkaline solution is used for aluminium etching, which does not attack the underlying zinc oxide. The whole structure is finally passivated by a sandwich of a silicon oxide and a silicon nitride layer on top. The passivation layers are deposited by PECVD at low temperature. An oxygen rich plasma process (SiH_4/N_2O) is used to prevent hydrogen from diffusing into the zinc oxide. The silicon oxide layer isolates the zinc oxide from the hydrogen rich silicon nitride plasma process (SiH_4/NH_3); the additional nitride is needed as a more reliable, very dense passivation layer to guarantee long time stability of the zinc oxide.

In a process modification, PECVD-silicon oxide is first deposited on the zinc oxide, before the aluminium metallization and the final nitride passivation layer is put on top. The oxide separates the metal from the zinc oxide, which results in improved piezoelectric properties.

The wafer frontside is then masked by photoresist, and the contact holes and openings for the final trenching process are opened.

Wet etching membranes from the wafer backside is done in a hot KOH-solution using frontside protection. The remaining membrane thickness is controlled by etching time and visual inspection. After careful cleaning of the wafers, the V-grooves are refilled with photoresist to stabilize the membranes. The deep trenching is done in a novel high density plasma etcher allowing anisotropic etching at a high rate and a high selectivity towards photoresist mask material.

The chips are then separated by sawing, the photoresist is removed using acetone and an oxygen plasma stripper or concentrated nitrous acid.

Resonant force sensor

The sensor described in this section consists of four piezoelectrically active ZnO-areas of same size and thickness (*a-d*, see fig.1) over the length of the beam in contrast to [2,6], where only two piezoelectric areas are used (area *a* and *d*).

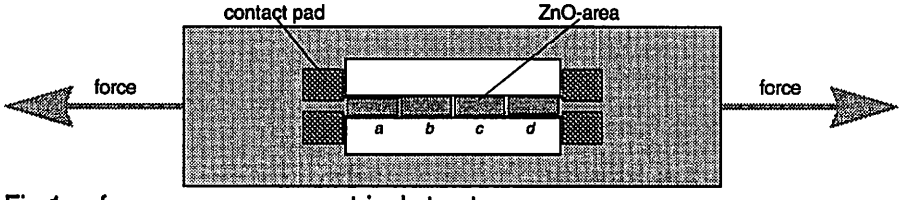

Fig.1: force sensor - geometrical structure.

The sensor is driven as a two-port-element in a way that some of the ZnO-areas excite the vibration of the beam and other(s) detect it. Depending on the relative positions of the areas for excitation and detection there is a different behaviour of the electrical signal transmission from one port to the other.

In the fundamental out-of-plane vibration mode the outer ZnO (*a* or *d*) areas will be stressed if the inner ones (*b* or *c*) will be strained, and vice versa. This results in different signs of the piezoelectric charge produced in the ZnO-areas.

First we will look at the excitation and detection of beam vibrations by the outer ZnO areas corresponding to the operating mode of sensors described by van Mullem *et al.* [6]. In this case the inner two areas (*b,c*) of the four-area-sensor are unconnected. Figure 2 shows a typical gain-phase-curve of a resonant sensor driven with a sinusoidal signal of constant amplitude (100mV) and variable frequency.

The received signal U_1 is compared in gain and phase φ with the excitation signal U_0 and is plotted vs. frequency.

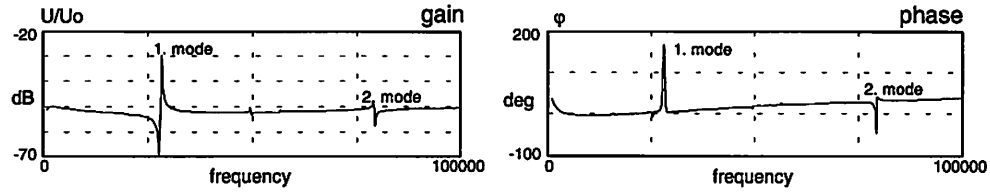

Fig.2: Measured gain-phase-curve of a resonant sensor driven and detected by outer areas (*a→d*).

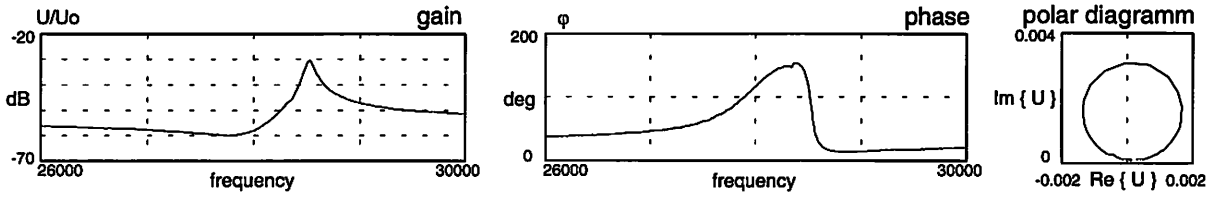

Fig.3: Measured electrical behavior of a resonant sensor near the first vibration mode driven and detected by outer ZnO-areas (*a→d*).

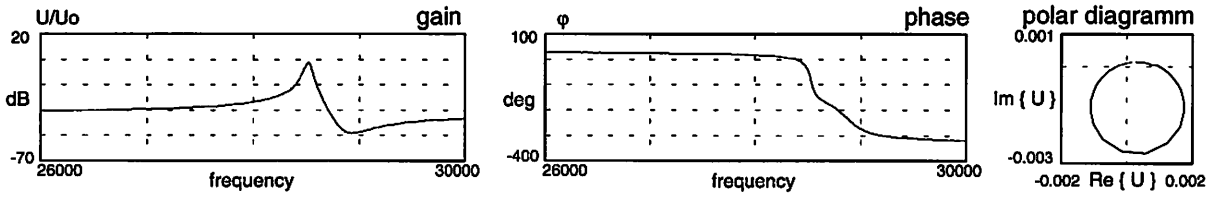

Fig.4: Measured gain-phase-curve of a resonant sensor near the first vibration mode detected by an inner ZnO-area (*a→c*).

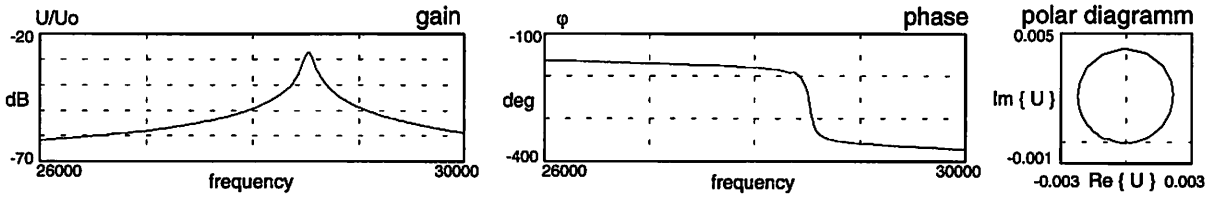

Fig.5: Measured gain-phase-curve of a dual driven resonant sensor near the first vibration mode (*a+b →d*).

In fig.3, the range of the first vibration mode is shown. Another operating mode for excitation and detection of beam vibrations is to use ZnO-areas unsymmetrically located on the beam (e.g. an outer versa an inner area) (fig.4). The third operating mode was a dual driven vibration. In this case two neighbouring ZnO-areas located at the end of the beam were driven with a phase shift of 180° (*a+b*). The vibration was detected by the second outer area (*d*) (fig.5).

Discussion

In general, the behaviour of mechanical resonators can be represented as a circle in the complex plane in the third and fourth quadrant with its "footpoint" in the origin of the plane. At frequencies below the point of resonance the complex transmission signal U=U(f)*exp(jφ(f)) assumes a real value. Near the resonance frequency the transmission signal reaches a maximum if the quality factor is greater than 1 corresponding to a phase shift of -90°. In the higher frequency region its magnitude decreases sharply and the phase shifts to -180°.

The presented curves are a superposition of the mechanically induced piezoelectrical signals and of electrical crosstalk. The electrical crosstalk is nearly a constant in the relevant frequency range of only a few hundred Hertz near the point of resonance. Its value reaches -50dB at 20° phase angle

depending on the input impedance of the connected amplifier. Van Mullem *et al.* [3] have thoroughly discussed this crosstalk.

In the operating mode shown in fig.2 and 3 (excitation and detection by outer areas *a,d* and also described by van Mullem *et al.* [6]) the circle representing the mechanical response is found in the first and second quadrant of the complex plane because the inverse piezoelectric effect changes the sign of the signal. The electrical crosstalk shifts the footpoint of this circle away from the origin of the complex plane. For this reason the gain curve of the resonant sensor reaches a minimum first and then a maximum with increasing frequency.

In the unsymmetrical driving mode ($a \rightarrow c$ or $b \rightarrow d$) the "mechanical" circle keeps its original location in the third and fourth quadrant. Because of electrical crosstalk similar to the situation described above, the footpoint of this circle will be shifted into the first quadrant and the circle itself now includes the origin (fig.4). In the electrical behaviour of the resonant sensor the maximum is now reached before the minimum with increasing frequency. The phase changes a total of 360° from about 20° via -70° at the point of resonance down to -340°.

As shown in fig.5, with the dual-drive mode the footpoint of the "mechanical" circle coincides with the origin. Therefore we conclude that electrical crosstalk is strongly supressed in this drive mode due to the fact that the electrical currents responsible for crosstalk compensate between the two areas driven at counterphase.

A similar improvement can be achieved by taking the signal difference from the outer and inner piezoelectrical pickup field. However, this requires a difference amplifier with a high common mode suppression.

In both cases the vibration mode (fundamental or second mode) can be selected by controlling the phase shift of the electric feedback loop (-90° for the fundamental mode and -270° for second vibration mode by using the outer evaluating ZnO area).

Acknowledgements

This work was supported by the Bundesministerium für Forschung und Technologie (BMFT) under contract number 13 AS 0117 / 0118. The authors would like to thank Prof. Dr. S. Büttgenbach for his assistance.

References

1 G. Stemme, Resonant silicon sensors, *J. Micromech. Microeng. 1* (1991), p. 113-125.

2 H. A. C. Tilmans, M. Elwenspoek and J. H. J. Fluitman, Micro resonant force gauges, *Sensors and actuators A, 30, no. 1-2* (1992) 35-53.

3 C. J. van Mullem, H. A. C. Tilmans, A. J. Mouthaan and J. H. J. Fluitman, Electrical cross-talk in two-port resonators - the resonant silicon beam force sensor, *Sensors and Actuators A, 31* (1992) 168-173.

4 F.R.Blom, D.J.Yntema, F.C.M. van de Pol, M. Elwenspoek, J.H.J. Fluitman and Th.J.A. Popma, Thin-film ZnO as micromechanical actuator at low frequencies, *Sensors and Actuators A, 21-23* (1990), p. 226-228.

5 F.R. Blom, F.C.M. van de Pol, G. Bauhuis and Th.J.A. Popma, R.F.-planar magnetron sputtered ZnO-films - part II: electrical properties, *Thin Solid Films 204* (1991), p. 365-376.

6 C. J. van Mullem, F.R. Blom, J. H. J. Fluitman and M. Elwenspoek, Piezoelectrically driven silicon beam force sensor, *Sensors and Actuators A, 25-27* (1991) p.379-383.